ARCHIVES
of
FOUNDRY ENGINEERING

ISSN (2299-2944)

10.24425/afe.2024.151287

Published quarterly as the organ of the Foundry Commission of the Polish Academy of Sciences

Abrasive Wear Resistance of Nodular Cast Iron After Selected Surface Heat and Thermochemical Treatment Processes

C. Baron [a], M. Stawarz [a], A. Studnicki [a], J. Jezierski [a, *], T. Wróbel [a], R. Dojka [b], M. Lenert [a, b], K. Piasecki [a, b]

[a] Silesian University of Technology, Department of Foundry Engineering, Towarowa 7, 44-100 Gliwice, Poland
[b] Odlewnia RAFAMET Sp. z o.o., ul. Staszica 1, 47-420 Kuźnia Raciborska, Poland
* Corresponding author: E-mail address: jan.jezierski@polsl.pl

Received 23.05.2024; accepted in revised form 06.07.2024; available online 22.07.2024

Abstract

The article presents the test results on the technology of surface hardening of castings from unalloyed and low-alloy nodular cast iron using the method of surface heat treatment, i.e., induction surface hardening and methods of thermochemical treatment, i.e. gas nitriding, nitrocarburizing, and nitrocarburizing with oxidation. The scope of research included macro- and microhardness measurements using Rockwell and Vickers methods, respectively, as well as metallographic microscopic examinations using a light microscope. Furthermore, abrasive wear resistance tests were performed using the pin-on-disk method in the friction pair of nodular cast iron – SiC abrasive paper and the reciprocating method in the friction pair of nodular cast iron – unalloyed steel. Analysis of the test results shows that the size and depth of surface layer hardening strongly depend on the chemical composition of the nodular cast iron, determining its hardenability and its ability to create diffusion layers. Medium induction surface hardening made it possible to strengthen the surface layer of the tested nodular cast irons to the level of 700 HV0.5 with a hardening depth of up to approximately 4000µm, while various variants of thermochemical treatment provided surface hardness of up to 750 HV0.5 with a hardening depth of up to approximately 200µm. Furthermore, induction surface hardening increased the resistance to abrasive wear of nodular cast iron castings, depending on the test method, by an average of 70 and 45%, while thermochemical treatment on average by 15 and 60%.

Keywords: Surface hardening, Nitriding, Nitrocarburizing, Nitrocarburizing with oxidation, Abrasive wear

1. Introduction

Resistance to abrasion wear is one of the essential properties of engineering materials used to manufacture the working parts of many machines. The working parts of the machine operate in very different tribological systems that determine the appropriate selection of materials for these parts. Selection criteria depend on the actual wear mechanism, which is most often the sum of various individual wear mechanisms. In this case, the selection of the appropriate material is not as obvious and unambiguous as it appears. Eventually, the selection of a specific material resistant to tribological wear is determined by the dominant wear mechanism that occurs in the tribological system under consideration. The characteristics of the material developed as a result of the tribological wear resistance tests can help choose the right material. There is no single universal test method to determine resistance to tribological wear, as there are many types of tribological wear [1-9]. Each type of tribological wear often

requires the use of materials with specific properties, which allows us to say that there is no universal material resistant to all forms of tribological wear. For this reason, new test equipment for measuring wear in various tribological systems is constantly being developed, frequently characterized by one dominant wear mechanism, which can be helpful when choosing a material when we can define the dominant wear mechanism of the machine part under design. To minimize the risk of choosing an improper material, some machine parts manufacturers are equipped with test benches with a replica of the real machine [10-12] (e.g. pumps, crushers, mills, etc.), often smaller in size, using modern tools [13].

Nodular cast iron belongs to the group of casting engineering materials that exhibit very good mechanical properties [14-16]. For this reason, this material is willingly used for the manufacture of working machine parts in various industries [17-19] (mining, metallurgical, automotive, mechanical engineering, construction, etc.). Unfortunately, nodular cast iron cannot be classified as a material with high resistance to abrasive wear, especially in situations where the micro-cutting mechanism dominates [20-21].

This article describes research on improving the resistance to abrasive wear in specific tribological systems of selected nodular cast iron grades after surface heat treatment and thermochemical treatment.

2. Aim, methodology, and the scope of testing

The aim of the investigation was to determine the effect of selected processes of surface hardening of the surface layer of castings made of low-alloy nodular cast iron (melt W1 and W2) and unalloyed (melt W3 and W4) on wear resistance in various tribological systems.

Surface heat treatment covered induction surface hardening using various process parameters. This process made it possible to change the structure of the surface layer (to a depth of a few millimetres) of a sample made of the cast iron under test. Thermal chemical treatment included three processes: nitriding, nitrocarburizing, and nitrocarburizing with oxidation. These processes ensure a change in the structure of the subsurface layer of the sample only to a depth of about tens of micrometres.

Table 1 shows the short characteristics of the nodular cast irons under test. Detailed chemical compositions of nodular cast irons are the know-how, being the secret of the foundry – beneficiary of the project under which they were developed, and hence they are not provided. The tests were carried out using four types of cast iron, W1 and W3 were nodular cast irons with increased elongation (patent pending P.443934), while W2 and W4 were nodular cast irons with increased strength (patent pending P.443935). However, the ranges of the element concentrations in the studied nodular cast iron W1–W4 are given below [22]:

Gray cast iron grade GJS-700-4 comprises 0.30 to 0.50 wt.% Mn, 0.03 to 0.08 wt.% Mg, less than 0.05 wt.% Cr, and less than 0.01 wt.% V. Additionally, it contains 3.10 to 3.45 wt.% C, 2.35 to 2.75 wt.% Si, less than 1.10 wt.% Ni, less than 0.50 wt.% Mo, and 0.40 to 0.70 wt.% Cu.

Gray cast iron grade GJS-750-2 contains 0.35 to 0.55 wt.% Mn, 0.03 to 0.08 wt.% Mg, less than 0.05 wt.% Cr, and less than 0.01 wt.% V. It also includes 3.20 to 3.45 wt.% C, 2.35 to 2.65 wt.% Si, 0.7 to 1.50 wt.% Ni, 0.30 to 0.50 wt.% Mo, and 0.40 to 0.70 wt.% Cu.

Gray cast iron grade GJS-600-6 comprises 0.30 to 0.50 wt.% Mn, 0.03 to 0.08 wt.% Mg, less than 0.05 wt.% Cr, less than 0.01 wt.% V, less than 0.05 wt.% Ni, and less than 0.01 wt.% Mo. Additionally, it contains 3.10 to 3.45 wt.% C, 2.35 to 2.75 wt.% Si, and 0.40 to 0.70 wt.% Cu.

Gray cast iron grade GJS-650-3 contains 0.35 to 0.55 wt.% Mn, 0.03 to 0.08 wt.% Mg, less than 0.05 wt.% Cr, less than 0.01 wt.% V, less than 0.05 wt.% Ni, and less than 0.01 wt.% Mo. Additionally, it includes 3.20 to 3.45 wt.% C, 2.35 to 2.65 wt.% Si, and 0.40 to 0.70 wt.% Cu.

The surface hardening and thermochemical treatment test samples were prepared from test inputs obtained after melting in a crucible induction furnace with a capacity of 50 kg. The test samples were of the shape of a rectangular prism with dimensions of 30x25x65 mm (width x thickness x length). Figure 1 shows a trial ingot with marked locations of test sample cutouts.

Table 1.
Selected properties of the cast irons tested in the as-cast state

Melt	Grade	Hardness in the as-cast state, HB	UTS, MPa	Elongation, %
W1	GJS-700-4	269	803	4
W2	GJS-750-2	283	777	2
W3	GJS-600-6	283	649	6
W4	GJS-650-3	292	717	3

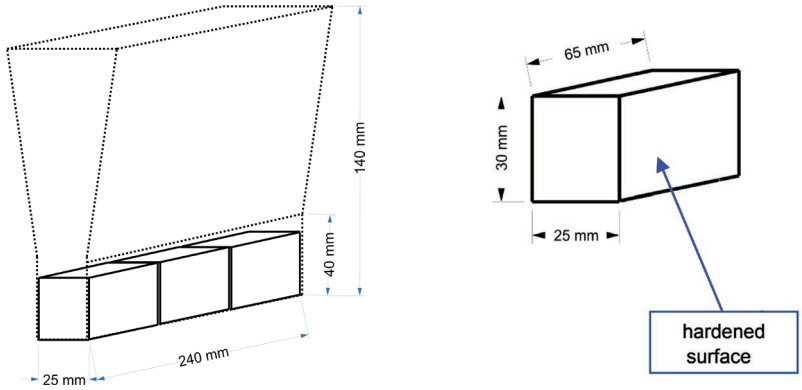

Fig. 1. Trial ingot and test sample

3. Hardening processes of the test sample surface layer

All activities related to the modification of the nodular cast iron surface layers aimed at increasing the hardness in the area exposed to abrasive wear, which was verified by using various experimental methods for the assessment of the resistance to abrasive wear. This article describes the melts made of selected nodular cast iron grades subjected to various heat treatment and thermochemical treatment processes, the aim of which was to significantly increase the hardness in the surface layer of the casting under test. The selected surface hardening methods differ in the thickness of the hardened layer that can be obtained, which may affect the applicability of these methods in different tribological systems.

3.1. Induction surface hardening

The induction surface hardening process was carried out for nodular cast iron samples with dimensions 35x25x65 mm. The hardening process was performed on opposite surfaces with the following dimensions: 35x65 mm. In the tests, an Elkon-made HI-10/50 induction surface hardening machine operated at an inductor supply frequency of 40.5 kHz (Fig. 2) was used. The nodular cast iron hardening process was carried out using the feed method, during which the inductor covered a small part of the heated sample zone, moving at speed V while heating subsequent zones. After leaving the inductor operating zone, the surface is heated to the austenitizing temperature of the nodular cast iron and was cooled by spraying a cooling liquid: 15% solution of Aqua Quench 260 polymer in water at a temperature of 25°C.

a) b)

Fig. 2. Induction surface hardening:
a) view of the HI-10/50 Elkon hardening machine,
b) view of the feed type sample hardening process (1-inductor, 2-sample, 3-sample holder, 4-cooling liquid)

As part of the test, the induction surface hardening of the nodular cast iron samples W1, W2, W3, and W4 was carried out, applying each time the power of 20 kW (I = 336 A) and using the hardening speeds V = 2.0; 2.5 and 3.0 mm/s.

A visual assessment of the quality of the hardened sample surfaces was performed and the hardness was measured with the Rockwell method using the universal hardness tester SBRV-100D by SUNPOC and an indenter in the form of a diamond cone with an apex angle of 120°, loaded with force 1,471 N (Rockwell HRC scale). Visual tests show that the surface of all cast iron samples after induction hardening was covered with a thin, dark layer of sediment from the polymer coolant component. The presence of the layer does not affect the technological suitability (the castings are dedicated for the specific, heavy duty conditions) of surface-hardened nodular cast iron. The parameters of the applied surface hardening process did not induce the presence of partial melting-type defects or cracks in any of the samples under test. Figure 3 shows an example of a set of test samples after surface hardening. Figure 4 shows the results of the surface hardness measurements of the samples, comparing them with the hardness of the test samples in the as-cast state.

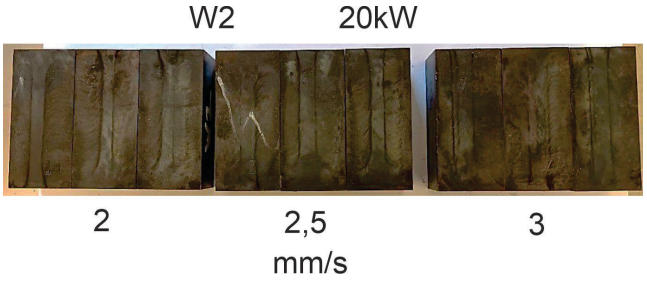

Fig. 3. Induction hardened surface of nodular cast iron W2 test samples at P = 20 kW and V = 2.0 mm/s, 2.5 mm/s and 3.0 mm/s

The scope of the study also included metallographic examinations of microsections after surface hardening of nodular cast iron samples, made by a standard method by grinding with abrasive papers with grit size ranging from 200 to 1000 and polishing by using a felt wheel with an aqueous mixture of Al_2O_3 using etching with Nital reagent with the following chemical composition: 10 cm^3 nitric acid + 100 cm^3 ethanol. To precisely determine the depth of hardening, microhardness measurements were carried out using the Vickers method with an FM 700 microhardness tester manufactured by FUTURE-TECH and an indenter in the form of a diamond pyramid loaded with 4.9 N operating 8 s (scale μHV0.5 with automatic conversion to HRC).

Figure 5 shows the microstructure of low-alloy nodular cast iron W1, in the area of the hardened layer, the tempered layer, the transition zone, and the un-hardened core, respectively.

For low-alloy nodular cast irons W1 and W2, regardless of the hardening rate used, the hardened layer contains a microstructure composed of nodular graphite in a martensitic matrix with a small amount of retained austenite. This type of hardened layer microstructure transitions directly into the microstructure of the unhardened core, which consists of nodular graphite in a pearlitic matrix with a small amount of ferrite. However, for unalloyed nodular cast irons W3 and W4, regardless of the hardening rate used, the hardened layer, similar to that of W1 and W2 cast irons, also has a microstructure composed of nodular graphite in a martensitic matrix with a small amount of retained austenite. Unlike W1 and W2 cast irons, the amount of martensite deeper in the hardened layer decreases, giving way to bainite and then to a mixture of bainite, pearlite, and ferrite. In the area of the unhardened core, no bainite was observed in the matrix of nodular graphite, but only pearlite with a small amount of ferrite.

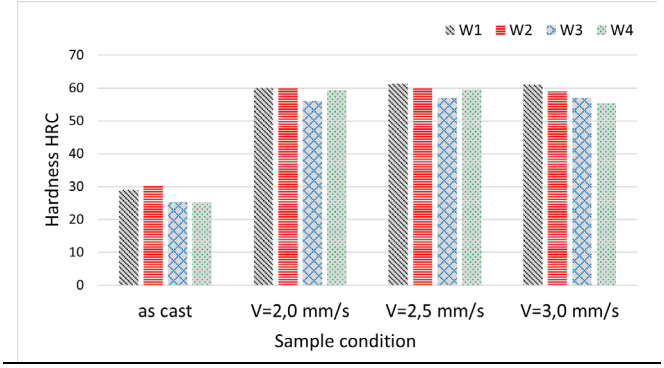

melt	as cast	V=2.0 mm/s	V=2.5 mm/s	V=3.0 mm/s
W1	29	60	61,3	61
W2	30,3	60	60	59
W3	25,3	56	57	57
W4	25,3	59,3	59,6	55,3

Fig. 4. Impact of the induction surface hardening process on the surface layer (HRC) hardness of the test samples

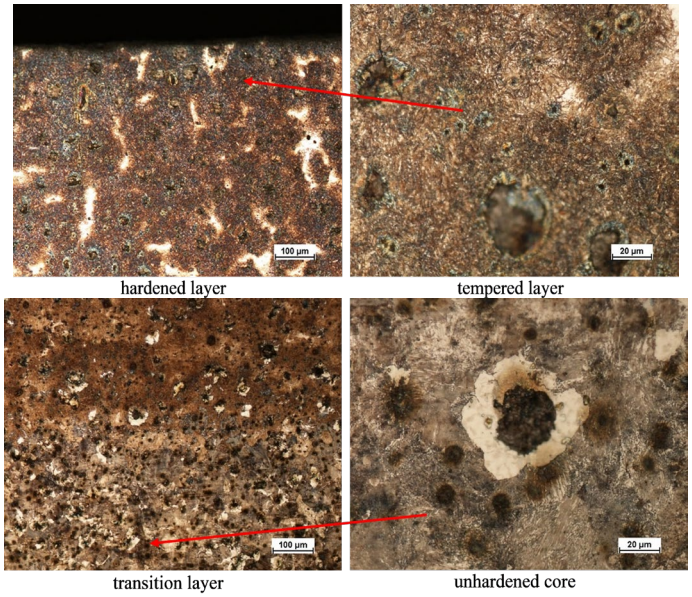

Fig. 5. Microstructure of nodular cast iron W1

Figure 6 shows the distribution of matrix microhardness measurements on the cross section of nodular cast iron W1 samples during the test under the condition after induction surface hardening at different speeds. The figure shows the lines defining the hardness of cast iron in the as-cast state (CS) and lines defining the adopted criteria for the minimum hardness of the hardened layer (DI55 and DI41) equal to 55 HRC and 41 HRC, respectively. Considering the above, it is easy to determine the thickness of the hardened layer that meets the adopted criteria. Tables 2 and 3 contain the summarized measurement results.

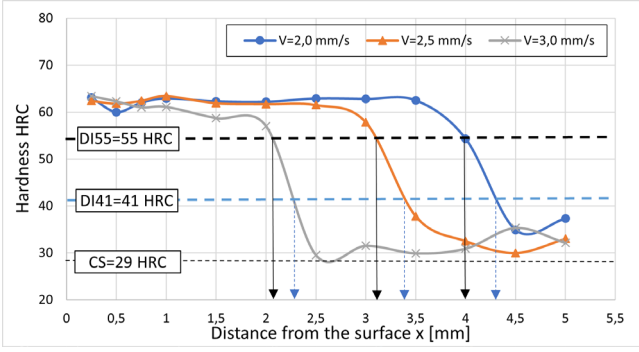

Fig. 6. Hardness distribution in the cross section of nodular cast iron samples W1 after induction surface hardening at different speeds

Table 2.
HRC hardness distribution in the cross section of nodular cast iron samples W1 and W2 after induction surface hardening at different speeds

x mm	W1			W2		
	V=2.0 mm/s	V=2.5 mm/s	V=3.0 mm/s	V=2.0 mm/s	V=2.5 mm/s	V=3.0 mm/s
0.25	63.1	62.4	63.4	63.3	62.4	62
0.5	60	61.8	62.3	63.6	60.7	58.7
0.75	62	62.4	61	63.5	60.9	61.2
1	62.9	63.4	61.1	63	61	60.6
1.5	62.3	61.9	58.7	62.7	58.5	52.5
2	62.2	61.7	57	59.8	57.4	52.2
2.5	62.9	61.5	29.5	62	60.3	36.9
3	62.8	57.8	31.5	60.2	34.2	29.8
3.5	62.5	37.8	29.9	47.6	31.8	33.5
4	54.3	32.5	30.9	34.8	30	33.6
4.5	34.9	30	35.3	32.2	33.7	30.8
5	37.3	33	32.1	31.6	34	31
DI55	**4.00 mm**	**3.10 mm**	**2.10 mm**	**3.25 mm**	**2.70 mm**	**1.50 mm**
DI41	**4.30 mm**	**3.40 mm**	**2.20 mm**	**3.75 mm**	**3.00 mm**	**2.40 mm**

Table 3
HRC hardness distribution in the cross section of nodular cast iron samples W3 and W4 after induction surface hardening at different speeds

x mm	W3			W4		
	V=2.0 mm/s	V=2.5 mm/s	V=3.0 mm/s	V=2.0 mm/s	V=2.5 mm/s	V=3.0 mm/s
0.25	62.2	61.5	60.3	63.7	59.4	58.7
0.5	63.5	63.6	53.9	62.8	60.8	51
0.75	63	63	50.9	61.9	58.6	50.3
1	63.4	60.5	45.6	61.1	59	50
1.5	61	60.4	36.7	61.9	52	47.7
2	59.5	47.9	21.6	54.6	48.8	38.8
2.5	50.3	34.7	24.7	57.6	29.2	33.3
3	46.7	32.1	27.8	33.7	30.7	27.8
3.5	25.5	29.5	22	32.8	28.1	30
4	27.3	28	25.3	28.2	27.5	26.3
4.5	26	30	26.6	31.9	26	26.8
5	22.3	27.7	24	38.7	25.8	17.1
DI55	**2.25 mm**	**1.75 mm**	**0.50 mm**	**2.60 mm**	**1.40 mm**	**0.40 mm**
DI41	**3.25 mm**	**2.25 mm**	**1.25 mm**	**2.80 mm**	**2.25 mm**	**1.80 mm**

Based on the analysis of the results obtained, it was found that for nodular cast iron W1 the hardened layer depth DI41 ranges from approximately 2.0 to approximately 4.0 mm, for nodular cast iron W2 DI ≈ 2.0÷3.5 mm, for nodular cast iron W3 DI ≈ 1.0÷3.0 mm while for nodular cast iron W4 DI ≈ 1.5÷2.5 mm. Therefore, it can be concluded that with the same process parameters for low-alloy nodular cast irons, i.e. W1 and W2, it is possible to obtain a greater depth of hardening compared to unalloyed nodular cast irons W3 and W4. Furthermore, despite the presence in the microstructure of unalloyed nodular cast irons, unlike low alloy nodular cast irons, a transition zone containing bainite, pearlite and ferrite, no “smoother transition” from the hardness characteristic of the hardened layer to the hardness specific to the unhardened core was found. It was also found that the value DI for all nodular cast iron samples under test strongly depends on the hardening rate, i.e. its increase causes a decrease in the depth of the hardened layer.

3.2. Nitriding, nitrocarburizing, and nitrocarburizing with oxidation

A set of test samples taken from nodular cast iron melts W1 to W4 was subjected to thermochemical treatment, under which three types of processes were performed, i.e. gas nitriding, nitrocarburizing and nitrocarburizing with oxidation, which were carried out at 540, 570 and 550°C, respectively with a duration 25, 4.5 and 8 h in an atmosphere of ammonia, ammonia and carbon dioxide, and ammonia and carbon dioxide with subsequent steam oxidation.

Figure 7 shows examples of test sample surfaces after the thermochemical treatment processes.

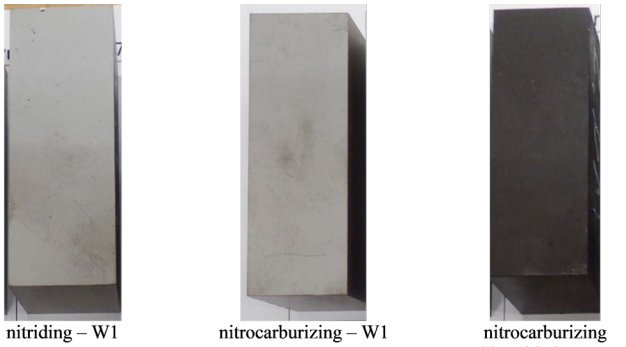

Fig. 7. Surfaces of test samples from the W1 melt after completing the thermochemical treatment processes

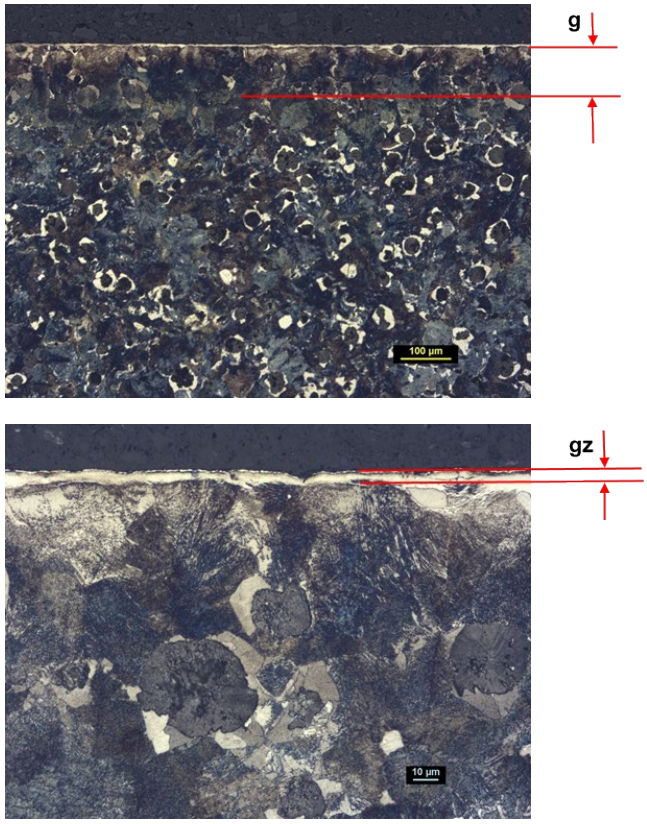

Fig. 8. Structure of the hardened layer after nitriding of nodular cast iron – W1 melt

A representative sample was selected for the complete testing of each set (both process and melt). The thickness measurements, Vickers microhardness measurements, and metallographic tests were performed for the layer obtained. Figure 8 shows the structure of the layer obtained after nitriding the nodular cast iron from melt W1, the layer thicknesses of the created compounds *gz* and the diffusion layer *g* determined according to the microhardness criterion of the core (HV0.2 of core + 50 HV0.2). Figure 9 shows an example of the microhardness distribution in the cross section of the melt sample W1. On the basis of the microhardness distribution, the parameters characterizing the layers obtained after the thermochemical treatment processes of the nodular cast irons under test were determined. They are listed in Table 4.

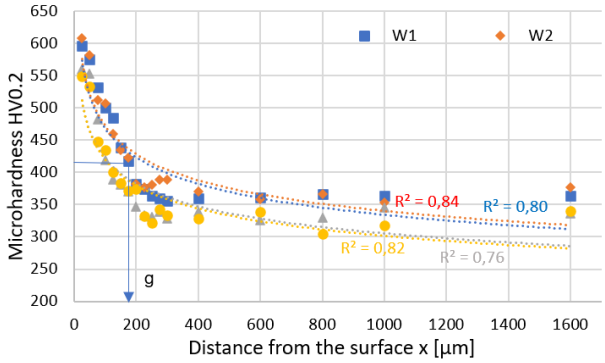

Fig. 9. Distribution of the microhardness of the nodular cast irons under test after nitriding

Analysis of the results obtained made it possible to find that, for low-alloy and unalloyed nodular cast irons, the highest degree of casting surface hardening is provided by the variant of gas nitrocarburizing with oxidation. Due to the presence of an increased concentration of Mo (up to 0.5%) in the chemical composition, the low-alloy nodular cast irons W1 and W2 after this type of thermochemical treatment obtain a hardness of up to approximately 750 HV, which is higher as compared to the value available for the unalloyed nodular cast irons W3 and W4, i.e. to approximately 700 HV. Furthermore, the hardening depth, which is the same as the thickness of the diffusion layer obtained in the thermochemical treatment process, ranges from approx. 100 to approx. 200µm, wherein regardless of the treatment variant, the upper limit is reached more often for low alloy cast iron W1 and W2, while the lower limit is reached for unalloyed cast irons W3 and W4.

4. Testing the abrasive wear of the samples

The resistance to abrasion is one of the important performance components of engineering materials. Abrasion can occur in many tribological systems that can be found in machines. The surface hardening of the nodular cast iron under test have provided very different parameters (thickness and hardness) of the layers obtained, which had to change the abrasion test results in the trials performed. It is commonly known that the hardness of the working part significantly affects the service life in the tribological system under consideration. The article presents the results of abrasion tests in two different tribological systems. In the system composed of metal (sample of nodular cast iron) – fixed abrasive grains (the countersample is an abrasive paper with a specific ceramic grit size), there was a significant difference in the hardness of these system components. The second system under analysis involves a metal sample (nodular cast iron) and a metal countersample (steel sheet). In this case, the tested sample

of nodular cast iron had a higher hardness compared to the steel sheet. For both abrasive wear tests, a sample with geometrical dimensions shown in Figure 10 was used. This sample was cut from the test sample after the surface hardening process.

Table 4.
Results of the hardened layer after thermochemical treatment of the nodular cast irons under test

Measured parameter	Melt	W1	W2	W3	W4
Nitriding					
Surface hardness	HV1	614 ÷ 652	631 ÷ 669	572 ÷ 611	521 ÷ 566
Surface microhardness	HV0.2	684 ÷ 741	705 ÷ 743	645 ÷ 695	608 ÷ 640
Diffusion layer thickness	g [μm]	180	170	130	140
Thickness of compounds layer	gz	4 ÷ 8	4 ÷ 10	4 ÷ 8	4 ÷ 7
Core microhardness	HV0.2	364	376	336	340
Core microhardness criterion (core + 50HV0.2)	CH	414	426	386	390
Nitrocarburizing					
Surface hardness	HV1	622 ÷ 652	602 ÷ 696	556 ÷ 629	511 ÷ 571
Surface microhardness	HV0.2	756 ÷ 855	780 ÷ 977	744 ÷ 828	765 ÷ 875
Diffusion layer thickness	g [μm]	150	140	90	110
Thickness of compounds layer	gz	6 ÷ 10	9 ÷ 13	6 ÷ 12	7 ÷ 14
Core microhardness	HV0.2	347	340	341	333
Core microhardness criterion (core + 50HV0.2)	CH	397	390	391	383
Nitrocarburizing with oxidation					
Surface hardness	HV1	678 ÷ 744	625 ÷ 728	623 694	567 ÷ 654
Surface microhardness	HV0.2	742 ÷ 956	873 ÷ 965	846 ÷ 917	810 ÷ 858
Diffusion layer thickness	g [μm]	140	180	140	120
Thickness of compounds layer	gz	6 ÷ 14	9 ÷ 16	7 ÷ 12	6 ÷ 15
Core microhardness	HV0.2	353	376	326	326
Core microhardness criterion (core + 50HV0.2)	CH	403	426	376	376

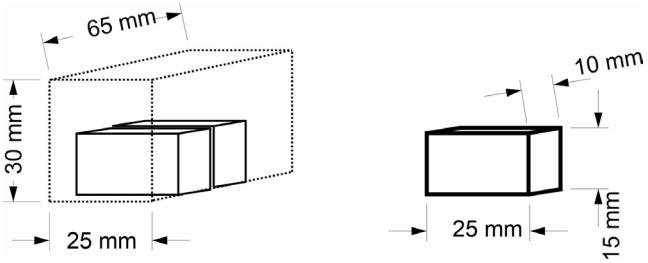

Fig. 10. Abrasive wear test sample and the method of collecting it from the test sample

4.1. Abrasion test in the system of metal-fixed abrasive grains using the pin-on-disk method

A test stand, developed in the Department of Foundry Engineering at the Silesian University of Technology, was utilized to assess abrasive wear. This apparatus is largely based on the pin-on-disk testing method, where a pin-shaped sample is pressed against a rotating disk to induce abrasive wear. In the Tribotester 3-POD, three samples are simultaneously pressed against a rotating disk, and these samples are also rotated within a specialized holder. Figure 11 illustrates both the operational diagram and the general appearance of this machine. The device tests three samples concurrently, with each sample mounted in a rotating holder that allows for individual pressure adjustments on the abrasive disk. The abrasive disk used is a sandpaper wheel with a specific grit size and type of abrasive grain. A new abrasive disk is employed for each set of samples. The direction of the abrasive disk's rotation is opposite to that of the sample holder. The machine's adjustable parameters include the rotations of the abrasive disk, rotations of the holder, sample pressure, type of abrasive disk, and the duration of the experiment [22].

The following operational parameters were used for the Tribotester 3-POD in the conducted tests:

- Sample dimensions: rectangular prism 10x15 (abraded surface) x 25 mm,
- Abrasive disk: abrasive paper 80, aluminum oxide,
- Abrasive disk speed: 170 rpm,
- Sample clamp speed: 300 rpm
- Load per sample: 230 G,
- Abrasion path per cycle: 800 m,
- Total abrasion path: 4800 m,
- Dry abrasion,
- Room temperature [22].

Weight loss was measured after each of the six measurement cycles (total distance travelled by the sample: 6x800 m = 4800 m) using scales with an accuracy of 0.001 g.

In this study, the Tribotester 3-POD stand was used to conduct abrasion tests on nodular cast iron in its as-cast state and after various surface treatments. The reference material used was a low-alloy steel resistant to abrasive wear, commercially known as CREUSABRO®8000 (marked as C8), with a hardness of 45 HRC. This reference material was consistently used for all abrasive wear tests performed on the Tribotester 3-POD

measuring stand at the Department of Foundry Engineering, Silesian University of Technology [22].

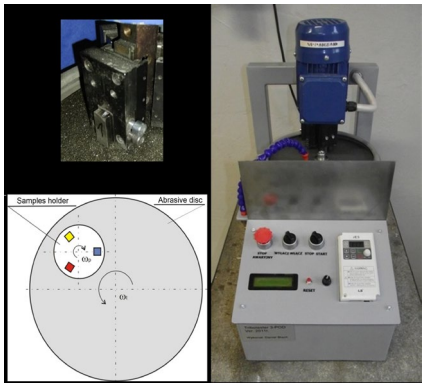

Fig. 11. Diagram of the machine operation and general view of the Tribotester 3-POD

Figure 12 shows the diagrams of abrasive wear in the full test cycle for nodular cast iron samples W1 and W3 in the as-cast state and after surface induction hardening at different induction hardening speeds. Figure 13 shows the summary of the total wear of all the nodular cast iron samples and the reference sample.

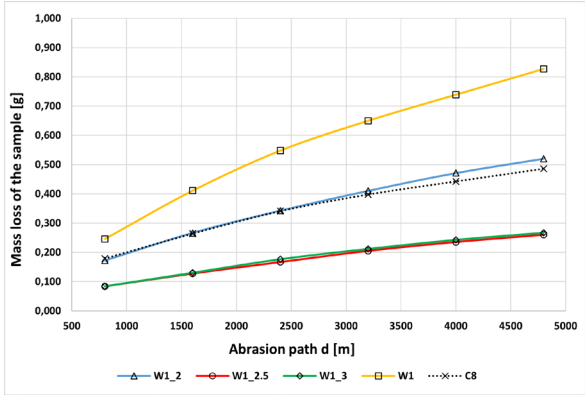

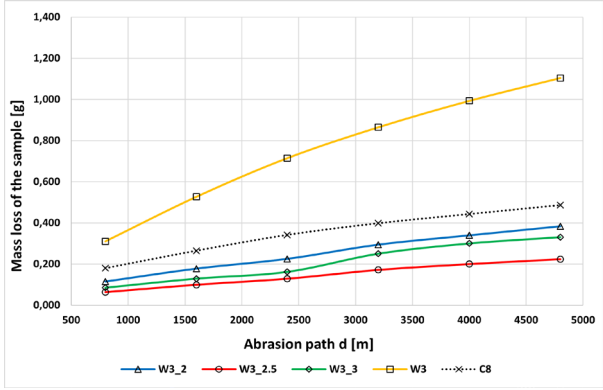

Fig. 12. Diagrams of abrasive wear as a function of the abrasion distance of samples for cast iron samples W1 (above) and W3 (below) after induction surface hardening and C8 reference in the metal-abrasive paper tribological system

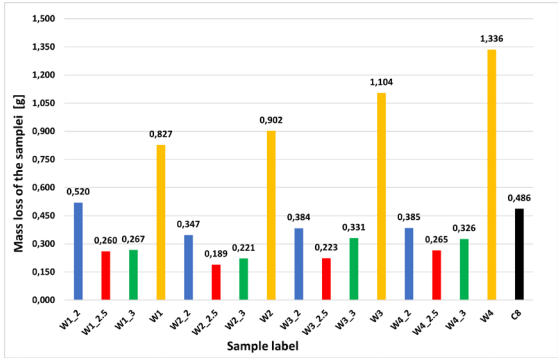

Fig. 13. Total wear of the tested samples of nodular cast iron W1–W4 in the as-cast state, after induction surface hardening and C8 reference sample in the metal-abrasive paper tribological system

Figure 14 shows the diagrams of abrasive wear in the full test cycle for nodular cast iron melts W1 and W3 in the as-cast state, after nitriding, nitrocarburizing, nitrocarburizing with oxidation and the C8 reference sample. Figure 15 shows the summary of total abrasive wear for all nodular cast iron samples in the as-cast state, after nitriding, nitrocarburizing, nitrocarburizing with oxidation and the C8 reference sample. Table 5 summarizes the measurement results of the total abrasive wear for the tested samples and determines the decrease in abrasive wear as compared to the as-cast state of the cast iron under test.

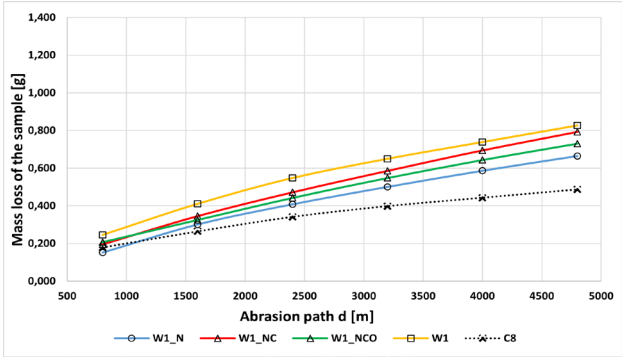

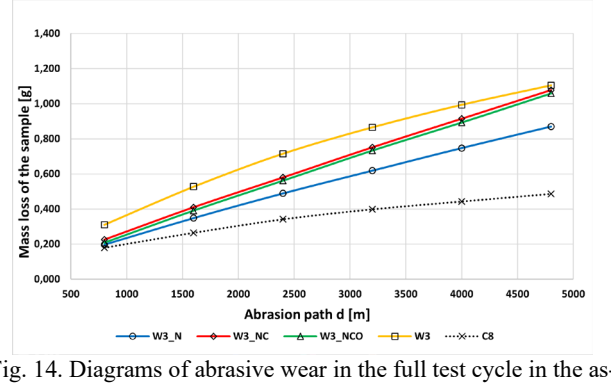

Fig. 14. Diagrams of abrasive wear in the full test cycle in the as-cast state, after nitriding, nitrocarburizing, nitrocarburizing with oxidation of samples for cast iron samples W1 (above) and W3 (below)and the C8 reference sample in the metal-abrasive paper tribological system

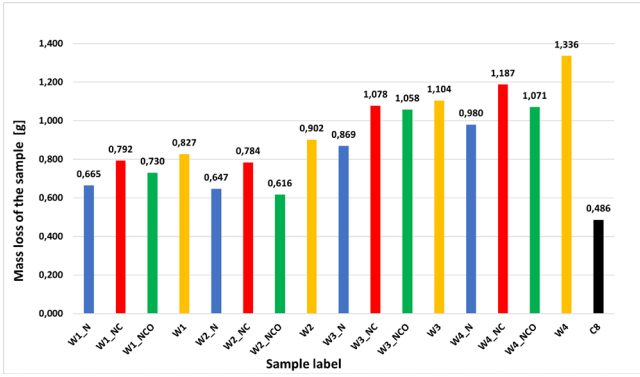

Fig. 15. Total wear of the tested samples of nodular cast iron W1–W4 in the as-cast state, after nitriding, nitrocarburizing, nitrocarburizing with oxidation, and the C8 reference sample in the metal-abrasive paper tribological system

Table 5.
Results of the measurement of abrasive wear for samples in a tribological system metal (sample) – fixed ceramic grains (abrasive paper)

Surface hardening			Diffusion hardening		
Sample	Δm, g	Wear reduction*, %	Sample	Δm, g	Wear reduction*, %
W1	0.827		W1	0.827	
W1_2	0.520	37%	W1_N	0.665	20%
W1_2.5	0.260	69%	W1_NC	0.792	4%
W1_3	0.267	68%	W1_NCO	0.730	12%
W2	0.902		W2	0.902	
W2_2	0.347	62%	W2_N	0.647	28%
W2_2.5	0.189	79%	W2_NC	0.784	13%
W2_3	0.221	75%	W2_NCO	0.616	32%
W3	1.104		W3	1.104	
W3_2	0.384	65%	W3_N	0.869	21%
W3_2.5	0.223	80%	W3_NC	1.078	2%
W3_3	0.331	76%	W3_NCO	1.058	4%
W4	1.336		W4	1.336	
W4_2	0.385	71%	W4_N	0.980	27%
W4_2.5	0.265	80%	W4_NC	1.187	11%
W4_3	0.326	76%	W4_NCO	1.071	20%
*cast iron reduction compared to as-cast cast iron state					

4.2 Reciprocating metal-to-metal abrasion test

A tribological machine was employed in the tests. This machine features a drive section, which includes an electric motor, belt transmission, gear transmission, and a crank mechanism. The operational section comprises a jaw chuck that executes a reciprocating (horizontal) motion and a vertically movable table, where a static force is applied using a lever system. Figure 16 presents the kinematic diagram and the general appearance of the machine.

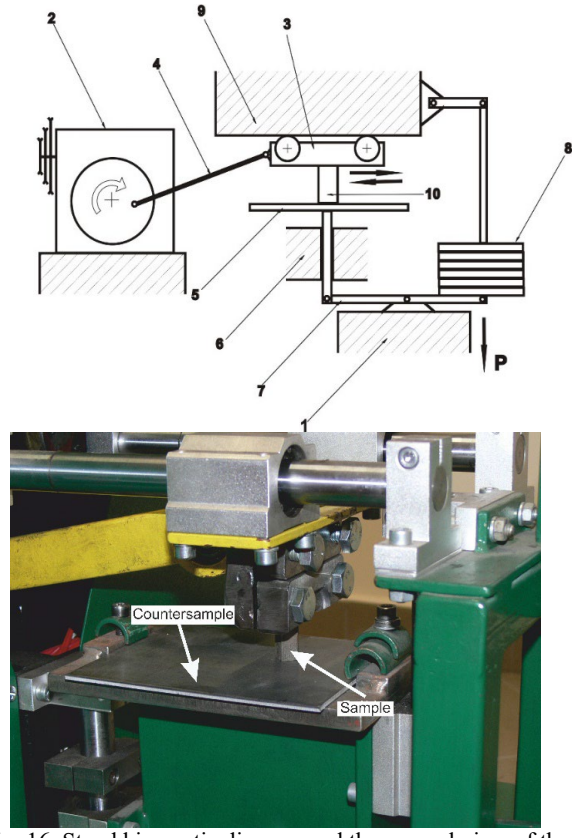

Fig. 16. Stand kinematic diagram and the general view of the machine 1-load-bearing frame, 2-reducer, 3-slider with a chuck, 4-connecting rod, 5-countersample, 6-set of countersample guides, 7-lever loading system, 8-set of weights, 9-set of slide guides, 10-sample

Samples with a cross-sectional area (abraded surface) of 10x15 mm and a height of 25 mm were examined. All samples were consistently mounted in the holder of the tribological machine. Each measurement cycle involved recording the weight loss of the material after completing 1500 cycles of the system's reciprocating motion, with each sample covering a distance of 150 m. A steel plate of grade S235 served as the countersample. The applied load on each sample was 50 N. Prior to testing, all samples were lapped to ensure full contact with the countersample. Weight loss was measured after each complete test cycle (150 m covered by the sample) using scales with an accuracy of 0.001 g. The scales were calibrated with mass standards before each test cycle to ensure accuracy, with a measurement error of ±0.001 g. During the tests, the air temperature in the laboratory was maintained at 21°C ±0.5°C [22].

Table 6 summarizes the measurement results of the abrasive wear for the tested samples and determines the decrease in the abrasive wear compared to the as-cast state of the cast iron under test. Figures 17 and 18 summarize the total wear of all samples of nodular cast iron tested in the as-cast state, after induction surface hardening, after nitriding, nitrocarburizing, and nitrocarburizing with oxidation.

Table 6.
Measurement results of abrasive wear for samples in a tribological system metal (sample) – metal (counter sample – steel plate grade S235).

Surface hardening			Diffusion hardening		
Sample	Δm, g	Wear reduction*, %	Sample	Δm, g	Wear reduction*, %
W1	0.014		W1	0.014	
W1_2	0.009	36%	W1_N	0.005	64%
W1_2.5	0.006	57%	W1_NC	0.010	29%
W1_3	0.007	50%	W1_NCO	0.006	57%
W2	0.012		W2	0.012	
W2_2	0.009	25%	W2_N	0.004	67%
W2_2.5	0.005	58%	W2_NC	0.004	67%
W2_3	0.007	42%	W2_NCO	0.008	33%
W3	0.021		W3	0.021	
W3_2	0.011	48%	W3_N	0.007	67%
W3_2.5	0.009	57%	W3_NC	0.005	76%
W3_3	0.009	57%	W3_NCO	0.010	52%
W4	0.019		W4	0.019	
W4_2	0.012	37%	W4_N	0.004	79%
W4_2.5	0.008	58%	W4_NC	0.005	74%
W4_3	0.014	26%	W4_NCO	0.010	47%

cast iron reduction compared to as-cast cast iron state

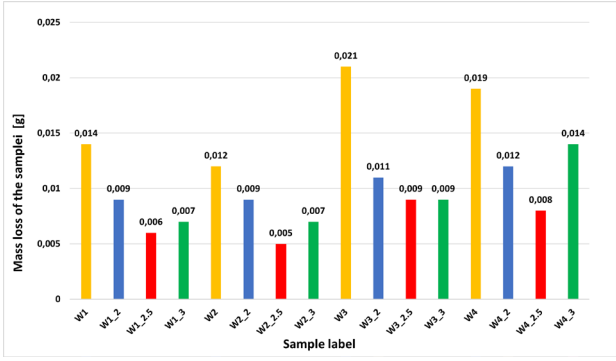

Fig. 17. Results of the test of the abrasion resistance of samples after hardening at different speeds (2.0, 2.5, 3.0 mm/s) for the sample reciprocating motion in the metal-to-metal tribological system

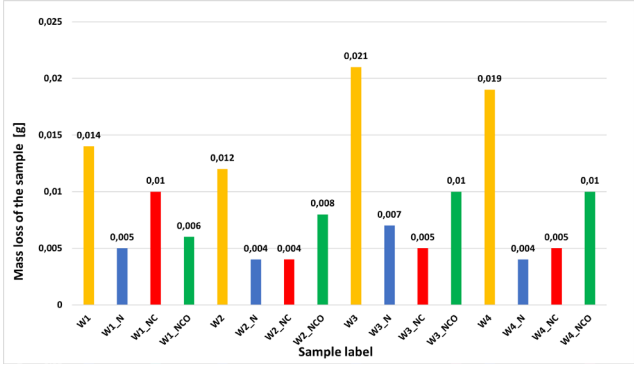

Fig. 18. Results of testing the abrasive wear of samples after nitriding (_N), nitrocarburizing (_NC), and nitrocarburizing with oxidation (_NCO) for the sample reciprocating motion in the metal-to-metal tribological system

5. Summary and conclusions

When analyzing the results of the abrasive wear test in the tribological system of metal-fixed abrasive grains, it is evident that surface hardening treatment significantly improves the resistance to abrasive wear of the tested nodular cast iron. It is also clear that there is an optimal hardening speed (2.5 mm/s), which maximizes abrasion resistance. Based on the induction surface hardening tests, a cast iron sample from the W2 melt can be selected to achieve the best abrasion resistance regardless of the surface hardening parameters, even though it was not the best in its as-cast state. In some cases, an improvement in abrasion resistance of up to 80% was observed compared to the as-cast state of the tested cast iron (W2, W3, and W4 melts). The high hardness of the hardened layer of nodular cast iron and the several millimetre thickness of this layer subjected to the abrasion test with ceramic grains play a significant role.

If the surface layer hardening of nodular cast iron was performed using diffusion hardening methods, the abrasion resistance increased by a maximum of about 20% compared to the as-cast state, with the increase often being only a few percent. Although the hardness of the layer achieved through diffusion hardening was high, its thickness was around 100 µm. This limited thickness likely contributed to the material's low abrasion resistance in the analyzed tribological system. It should be noted that the hardness of the surface layers obtained through both induction surface hardening and diffusion hardening methods for the tested nodular cast iron does not significantly enhance abrasion resistance in the metal-ceramic grain combination (with the ceramic grains used in the abrasion test having a Mohs hardness of approximately 9.2). Instead, these methods merely slow the rate of wear. In this context, the thickness of the hardened layer plays a crucial role.

Abrasive wear tests in the metal-to-metal tribological system for nodular cast iron, hardened by surface or diffusion methods, showed similar abrasion resistance. The countersample used had a hardness of about 200 HB, much lower than the analyzed layers, leading to positive results. Frequently, wear reduction exceeded 50% compared to the untreated nodular cast iron (without heat or thermochemical processing).

Based on the tests, the following conclusions were drawn:

1. The hardening treatment of the working part made of the tested nodular cast irons is justified only if the tribological system of the cooperating working parts is known.
2. If the tribological system includes a part with hardness much higher than that of the layer generated in nodular cast iron, the use of thin layers (diffusion hardening) becomes unjustified. In such cases, the use of thicker layers (surface hardening) will only reduce the rate of abrasive wear of the analyzed part.
3. Induction surface hardening with properly selected process parameters can significantly improve the resistance to abrasive wear in the tested tribological systems, especially for unalloyed nodular cast irons.
4. Diffusion hardening significantly increases the resistance to abrasive wear in the metal-to-metal tribological system if the hardness of the second working part does not exceed the hardness of the hardened layer. The layer of compounds with high microhardness (> 800 HV0.2) can be fully

utilized in the hardened layer, but the thickness of this layer is low (approximately 10 μm).

Acknowledgments

The article was prepared during the implementation of a project co-financed by the NCBiR (National Center for Research and Development) under the title: Development of an innovative manufacturing technology for large-size castings made of nodular cast iron with special properties in Full Mold technology, dedicated to the production of stamping tools in the automotive sector No. POiR.01.01.01.-00-0013/20.

References

[1] Pan, C., Gu, Y., Chang, J. & Wang, C. (2023). Recent patents on friction and wear tester. *Recent Patents on Engineering*. 17(4), 86-102. DOI:10.2174/1872212117666220621103655.

[2] Yang, Z., Ye, S., Wang, Z., Li, Z. & Li. W. (2023). Experimental and simulation study on braking noise characteristics and noise reduction strategies of the friction pair between the SiCp/A356 brake disc and the synthetic pad. *Engineering Failure Analysis*. 145, 1-20, 107017. https://doi.org/10.1016/j.engfailanal.2022.107017.

[3] Wang, K., Zhang, Z., Dandu, R.S.B. & Cai. W. (2023). Understanding tribocorrosion of aluminum at the crystal level. *Acta Materialia*. 245, 1-13, 118639. DOI:10.1016/j.actamat.2022.118639.

[4] Jakobsen, P.D., Langmaack, L., Dahl, F. & Breivik. T. (2013). Development of the soft ground abrasion tester (SGAT) to predict TBM tool wear, torque and thrust. *Tunneling and Underground Space Technology*. 38, 398-408. DOI:10.1016/j.tust.2013.07.021.

[5] Tiruvenkadam, N., Thyla, P.R. Senthil Kumar, M., Kader, N.A., Pradeep, V.K., Vishnu Kumar, R., Sasikumar, N. (2013). Development of multipurpose reciprocating wear tester under various environmental parameters. In International Conference on Energy Efficient Technologies for Sustainability, 10 – 12 April 2013 (pp. 213 – 216). Nagercoil, India. DOI:10.1109/ICEETS.2013.6533384.

[6] Guanzhang, H., Xiaojing, Y., Yilin, C. & Jie, D. (2011). Development of a system for measuring the variation of friction force on reciprocating wear tester. In Third International Conference on Measuring Technology and Mechatronics Automation, 6-7 January 2011 (Vol. 1, pp. 1045-1049). DOI:10.1109/ICMTMA.2011.262.

[7] Vasquez, H., Lozano, K., Soto, V. & Rocha, A. (2008). Design of a wear tester for nano-reinforced polymer composites. *Measurement.* 41(8), 870-877. DOI:10.1016/j.measurement.2007.12.003.

[8] Wei, R., Wilbur, P.J., Sampath, W.S., Williamson, D.L., Qu, Y. & Wang, L. (1990). Tribological studies of ion-implanted steel constituents using an oscillating pin-on-disk wear tester. *Journal of Tribology*. 112(1), 27-36. DOI:10.1115/1.2920227.

[9] Desale, G.R., Gandhi, B.K. & Jain, S.C. (2005). Improvement in the design of a pot tester to simulate erosion wear due to solid-liquid mixture. *Wear*. 259(1-6), 196-202. DOI:10.1016/j.wear.2005.02.068.

[10] Wang, X., Song, Y., Li, C., Zhang, Y. Ali, H.M., Sharma, S., Li, R. et al. (2023). Nanofluids application in machining: a comprehensive review. *International Journal of Advanced Manufacturing Technology*. 131(5-6), 3113-3164. DOI:10.1007/s00170-022-10767-2.

[11] De Stefano, M., Aliberti, S.M. & Ruggiero. A. (2022). (Bio) Tribocorrosion in dental implants: principles and techniques of investigation. *Applied Sciences.* 12(15), 1-16. DOI:10.3390/app12157421.

[12] Vilhena, L., Ferreira, F., Oliveira, J.C. & Ramalho. A. (2022). Rapid and easy assessment of friction and load-bearing capacity in thin coatings. *Electronics.* 11(3), 1-19, 296. DOI:10.3390/electronics11030296.

[13] Valigi, M.C., Logozzo, S. & Affatato, S. (2017). New challenges in tribology: wear assessment using 3D optical scanners. *Materials.* 10(5), 1-13, 548. DOI:10.3390/ma10050548.

[14] Dwulat, R., Janerka, K. & Grzesiak, K. (2021). The influence of final inoculation on the metallurgical quality of nodular cast iron. *Archives of Foundry Engineering*. 21(4), 5-14. DOI:10.24425/afe.2021.138673.

[15] Janerka, K., Kostrzewski, Ł., Stawarz, M. & Jezierski. J. (2020). The importance of SiC in the process of melting ductile iron with a variable content of charge materials. *Materials.* 13(5), 1-10, 1231. DOI:10.3390/ma13051231.

[16] Gumienny, G., Kurowska, B. & Fabian. P. (2020). Compacted graphite iron with the addition of tin. *Archives of Foundry Engineering*. 20(3), 15-20. DOI:10.24425/afe.2020.133323.

[17] Gunalan, M. & Anandeswaran, V.A. (2021). A holistic approach of developing new high strength cast iron for weight optimization. *SAE Techical Paper*. DOI:10.4271/2021-26-0244.

[18] Bendikiene, R., Bahdanovich, A., Cesnavicius, R., Ciuplys, A., Grigas, V., Jutas, A., Marmysh, D., Nasan, A., Shemet, L., Sherbakov, S. & Sosnovskiy, L. (2020). Tribo-fatigue behavior of austempered ductile iron monica as new structural material for rail-wheel system. *Medziagotyra.* 26(4), 432-437. DOI:10.5755/j01.ms.26.4.25384.

[19] [20] Zhu, Y., Keoleian, G.A. & Cooper. D.R. (2023). A parametric life cycle assessment model for ductile cast iron components. *Resources, Conservation and Recycling*. 189, 1-9, 106729. DOI:10.1016/j.resconrec.2022.106729.

[20] Molian, P.A. & Baldwin, M. (1987). Effects of single-pass laser heat treatment on erosion behavior of cast irons. *Wear*. 118(3), 319-327. DOI:10.1016/0043-1648(87)90075-5.

[21] Molian, P.A. & Baldwin. M. (1988). Wear behavior of laser surface-hardened gray and ductile cast irons. Part 2 erosive wear. *Journal of Tribology*. 110(3), 462-466. DOI:10.1115/1.3261651.

[22] Wróbel, T., Studnicki, A., Stawarz, M., Baron, Cz., Jezierski, J., Bartocha, D., Dojka, R., Opiela, J. & Lisiecki, A. (2024). Improving the abrasion resistance of nodular cast iron castings by remelting their surfaces by laser beam. *Materials*. 17(9), 1-17, 2095. https://doi.org/10.3390/ma17092095.